2008 IEEE International Conference on
Robotics and Automation
Pasadena, CA, USA, May 19-23, 2008

A Forearm Actuation Unit for an Upper Extremity Prosthesis

Thomas J. Withrow, *Member, IEEE,* Xiangrong Shen, Jason E. Mitchell, and Michael Goldfarb, *Member, IEEE*

***Abstract*— This paper presents the design of a 14 degree-of-motion forearm actuation unit for an upper extremity prosthesis. The forearm utilizes pneumatic type actuators which use the reaction products of a monopropellant gas generator as a working fluid. The use of pneumatic type actuators provides a near-human power density, such that the fourteen actuator forearm unit can deliver approximately one half of the force and power capability of a human arm, with a total package size that fits within the volumetric constraints of a 50th percentile female forearm (excluding the cartridge of liquid propellant). This paper describes the design of the forearm. The design has been fabricated, and experimental results are presented that demonstrate the closed-loop force tracking capability. An accompanying video further demonstrates the forearm performance.**

I. Introduction

THE authors are involved in an effort to develop a highly functional anthropomorphic upper extremity prosthesis. As part of this effort, the authors have developed a forearm actuation unit, which provides actuation for the three wrist degrees of freedom and eleven tendon actuators for the hand, all of which is contained within the geometric envelope of a 50th percentile female arm, which is shown in Figure 1. In order to provide human-like output with respect to force and speed, such a device must have a power density similar to that of a human forearm. In order to provide such power density, the authors utilize pneumatic type actuators. In order to power these actuators in a self-contained device, the authors are using a monopropellant gas generator, as described and characterized in [1-5]. Note that pneumatic-type upper extremity prostheses were developed in the 1960's (e.g., [6-12]). Those prostheses, however, had two significant limitations. First, they used CO_2 cartridges as the source of pressurized gas, which limited their energy capacity. Second, they used manual gas valves to control the movement of the arm, which did not afford good command tracking capability. In this work, we address both of these issues. The former issue is addressed by utilizing the monopropellant hydrogen peroxide rather than CO_2, which has between 5 and 12 times greater volumetric energy density (depending on the concentration of peroxide, ranging from 70% to 90%). Specifically, CO_2 transforms from liquid to gas via a phase transformation, whereas H_2O_2 transforms via an exothermic reaction. The latter contains significantly greater energy release, and therefore results in a greater source energy density. Regarding the second issue, that of servocontrol, the past few decades have provided small servomotors and significant advances in computer control, both of which enable the development of compact, computer-controlled servovalves, which in turn can provide accurate command tracking in a pneumatic-type servo system.

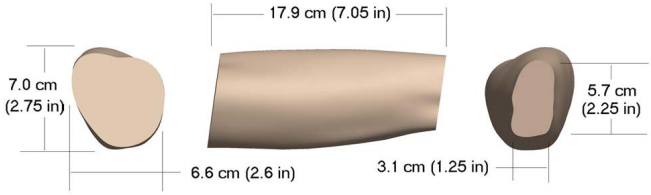

Fig. 1. Geometric envelope of 50th percentile female forearm.

II. Valve and Valve Bank Design

A solid model of the 14-actuator forearm design is shown in Fig. 2. A bank of 14 servovalves, which control the flow of gas to and from each cylinder, is located at the proximal end of the forearm. The required valve characteristics for the monopropellant-powered system are low-power operation, small size, and the ability to accommodate high-temperature gases. Servovalves with such characteristics, particularly at the required size, are commercially unavailable, thus necessitating custom design of the precision four-way valves.

Fig. 2. (left) Solid model of the forearm actuation unit within the volume constraint of a fifty percentile female volume. (right) Solid model of the actuation unit.

Manuscript received February 8, 2008. This work was supported in part by the U.S. Navy under Grant N66001-05-C-8045.

T. J. Withrow is with Vanderbilt University, Nashville, TN 37235 USA (e-mail: thomas.j.withrow@ vanderbilt.edu phone: 615-343-2782; fax: 615-343-6925).

X. Shen is with Vanderbilt University, Nashville, TN 37235 USA (e-mail: xiangrong.shen@ vanderbilt.edu).

J.E. Mitchell is with Vanderbilt University, Nashville, TN 37235 USA (e-mail: jason.mitchell@ vanderbilt.edu).

M.Goldfarb is with Vanderbilt University, Nashville, TN 37235 USA (e-mail: michael.goldfarb@ vanderbilt.edu).

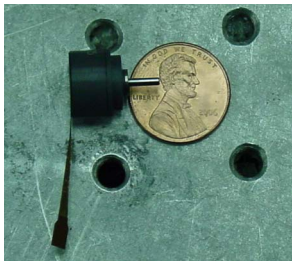

Fig. 3. Penny motor size relative to a penny.

Fig. 4. Stand-alone miniature servovalve, shown next to a AA-sized battery.

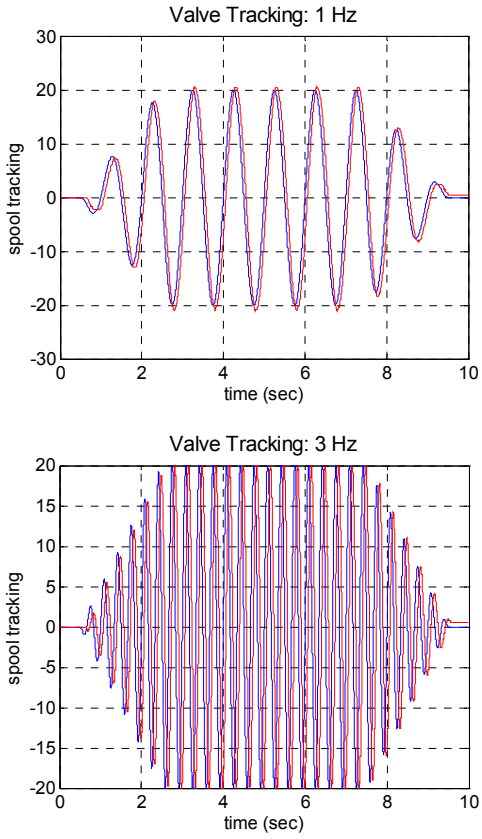

Fig. 5. Valve tracking at 2.07Mpa (300psi) for one and three Hertz commands.

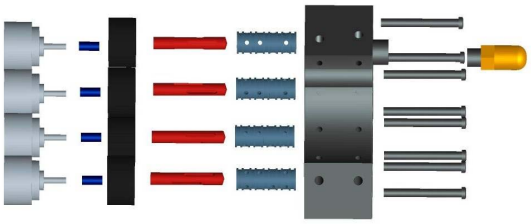

Fig. 6. Exploded view of four servovalve assemblies which are contained in the valve bank. From left to right the components are: servomotors (grey), shaft couplings (blue), housing and thermal isolators (black), valve spools (red), valve sleeves (blue), manifold (black), fasteners (grey), and muffler (gold).

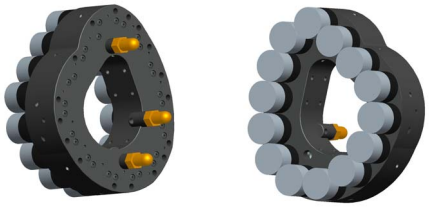

Fig. 7. (left) Solid model of valve bank which contains all 14 valves with the mufflers attached. (right) 14 motors attached to the valves within the valve bank.

The miniature custom servovalve design utilizes a rotary spool/sleeve pair, which are precision ground with a diametral clearance of 1 micron (XX gage quality). The spool is rotated within the sleeve by a brushless gearmotor package (Micromo penny motor model 1309W0007) (mass 2.7g, 12.4mm OD, body length 9.6mm) with a 259:1 gearhead, shown in Fig. 3. The complete valve package for a single valve is shown in Fig. 4. Experimental data indicating valve tracking capability at one Hertz and three Hertz is shown in Fig. 5. These valves are grouped in the arm in three valve banks, one of which is shown in an exploded view in Fig. 6. The full 14-valve bank consists of three sub-banks, grouped together as shown in Fig. 7. The miniature valves are the same as used in [1]. The perforce of this valve motor configuration are limited by the choice of the lightweight motor, with an alternative motor choice used with the exact same valve design have system tracking and bandwidth that is better by roughly an order of magnitude.

III. Actuator Sizing and Design

The pneumatic-type actuators were sized to deliver human-like performance, as outlined in Tables 1 and 3. The actuator size for a given prosthetic joint was chosen based on the output energy of its anatomical counterpart, which is defined by:

$$E = \tau\theta \qquad (1)$$

where τ is the average joint torque and θ is the angular range of motion of the joint. In conventional electromechanical designs, the power required at each joint generally

determines the actuator size. For gas actuation, however, the energy delivered is determined by the actuator volume whereas the power is dictated by the characteristics of the servovalve controlling the flow rate of gas through the cylinder. As such, the power produced at a given joint is essentially independent of the volume of the chosen actuator. Once the required energy for a given joint is determined, the volume of the pneumatic-type actuator is then determined by:

$$V = \frac{E}{P_s} \tag{2}$$

where P_s is the supply pressure of the working gas and V is the displaced volume of the actuator. The supply pressure for the prosthesis prototype is 2.1 MPa (300 psi). Table 1 summarizes the requirements for the three wrist degrees of freedom.

TABLE 1
FOREARM REQUIREMENTS

DOF	TORQUE (NM)	ROM (°)	ENERGY (J)	REQUIRED ACTUATOR VOLUME (CC)
Wrist Flex/Ext	4.5	170	13.4	6.5
Wrist Ab/Ad	4.5	60	4.73	2.3
Wrist Pro/Sup	4.2	150	11.1	5.3

After computing the required volume for a given actuator, the bore and stroke of the actuator can then be determined based on the required range-of-motion, the linkage design, and the constraint that the prosthesis design should fit within the anatomical envelope of the human arm. The predominant constraint with respect to the forearm design was fitting the actuators within the available forearm length. As such, each actuator was chosen to provide the requisite energy with the smallest overall actuator length (stroke plus additional length due to endcaps/ports). Table 2 summarizes the specifications of the actuators chosen for the prosthesis forearm and shows the ratios of the actual to desired actuator volumes for each degree of motion. This ratio provides an indirect measure of the additional actuator energy available to overcome the friction in each DOF (e.g., joint friction, cylinder seal friction, etc.).

TABLE 2
FOREARM ACTUATOR SPECIFICATIONS

DOF	STROKE (CM)	BORE (CM)	ACTUATOR DISPLACED VOLUME (CC)	ACTUATOR/REQUIRED DISPLACED VOLUME (CC)
Wrist Flex/Ext	5.1	1.4	8.1	**1.25**
Wrist Ab/Ad	3.8	1.4	6.1	**2.65**
Wrist Pro/Sup	3.8	1.4	6.1	**1.15**

Pronation/supination of the wrist is actuated by rotating the entire forearm relative to the supporting proximal forearm tube using a variant of a leadscrew assembly, the design of which is shown in Fig. 8. The design consists of proximal and distal forearms supported by a pair of flanged bearings (GGB models BB0808DU and BB1007DU) to allow rotation of the distal forearm relative to the proximal portion of the prosthesis while also providing for thrust load bearing. The proximal forearm tube includes a helical slot which acts as the leadscrew in the design. The distal forearm houses a rotating cylinder (Bimba model 021.5-DXPV) and includes a straight slot collinear with the helical slot of the proximal forearm tube. An orthogonally positioned PEEK crosspiece provides for relative rotation of the proximal/distal forearm pieces. As the cylinder rod is displaced, the PEEK crosspiece slides within the helical/straight slots of the proximal/distal forearm resulting in rotation of the distal forearm relative to its proximal counterpart with a total range of motion of 95°.

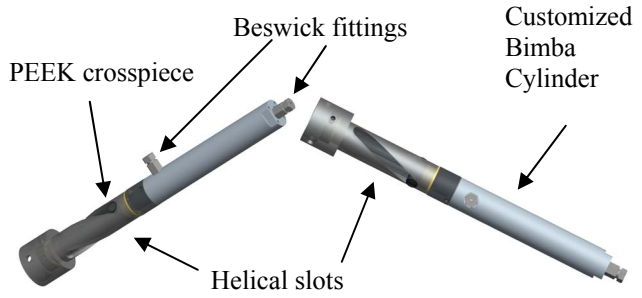

Fig. 8. Solid model of rotating wrist pronation/supination cylinder with PEEK crosspiece and the proximal forearm tube with helical slot.

Wrist flexion/extension and abduction/adduction, shown in the solid model of Fig. 9, are actuated with a pair of modified cylinders (Bimba models 022-DXPV and 021.5-DXPV). The linkage of these two wrist cylinders to the hand should allow for uncoupled motion between the ab/adduction cylinders and the flex/extension cylinders.

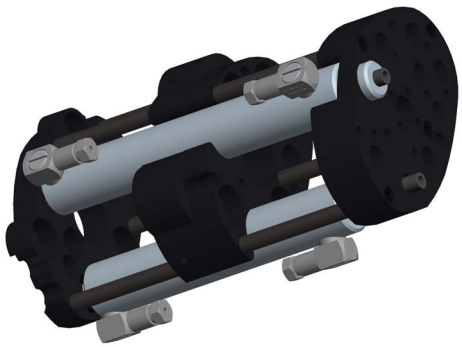

Fig. 9. Lateral view of solid model of wrist flexion/extension and abduction/adduction cylinders within the two hand actuator clusters (with the hand actuators removed). The flexion/extension cylinder is to the left in the model.

With respect to sizing the actuation for the hand, the energy was determined based on the desired exertion force

and range of motion for the finger and the thumb. For finger flexion, the energy is based on a force of 40 N over a finger-tip range of motion of 10 cm. The energy for thumb flexion is determined by a tip force of 60 N over 10 cm of motion, and that for thumb abduction/adduction is given by a force of 40 N over 8.5 cm of motion. Table 3 summarizes the requirements for the hand actuators, including force, range of motion, energy components, and required actuator volume.

TABLE 3
HAND ACTUATOR REQUIREMENTS

DOF	FORCE (N)	ROM (CM)	ENERGY (J)	REQUIRED ACTUATOR VOLUME (CC)
Finger flexion	40	10	4.0	**1.9**
Thumb flexion	60	10	6.0	**2.9**
Thumb ab/ad	40	8.5	3.4	**1.6**

The eleven actuators for the hand are heavily modified Bimba model 012-DV (n=9) and Bimba model 0072-DV cylinders (n=2). To aid in the compact nature of the design, the ends of the cylinders are removed and replaced with two sets of customized common end plates. The actuators are arranged in a double stacked configuration, in-line with the longitudinal axis of the forearm. Each of the two sets of end plates is held securely by four tie rods that are common to the cylinders for that set of end plates. The sealing and porting for the cylinder clusters occurs in the end plate and allows for a simpler and more compact actuator package, as seen in Fig 10.

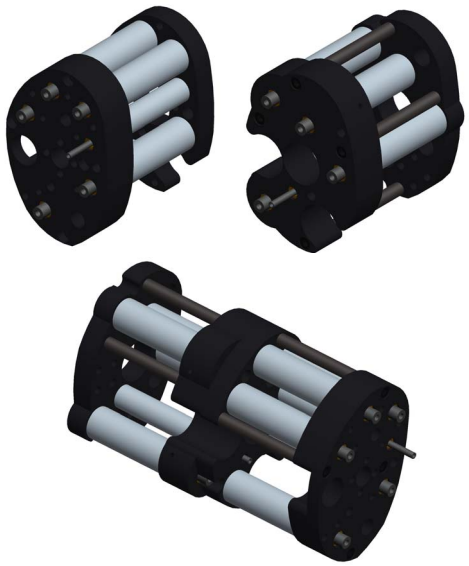

Fig. 10. Solid model of the two hand actuator clusters. (top) Medial view of the two separate actuator clusters with all 11 hand actuators. (bottom) Lateral view of the double-stacked configuration. All three images without the wrist cylinders.

TABLE 4
HAND ACTUATOR SPECIFICATIONS

DOF	STROKE (CM)	BORE (CM)	ACTUATOR DISPLACED VOLUME (CC)
n=9	3.8	1.1	**3.6**
n=2	3.8	0.8	**1.9**

The hand actuator specifications are summarized in Table 4. Note that the larger cylinders provide 1.6 times the force as the smaller cylinders.

Fig. 11 shows the fabricated complete actuation unit mounted on the proximal forearm tube with the motors, valves, 1.59mm (1/16") tubing with compression fittings (Beswick). The complete actuation unit has a total mass of 930g (2.05lb).

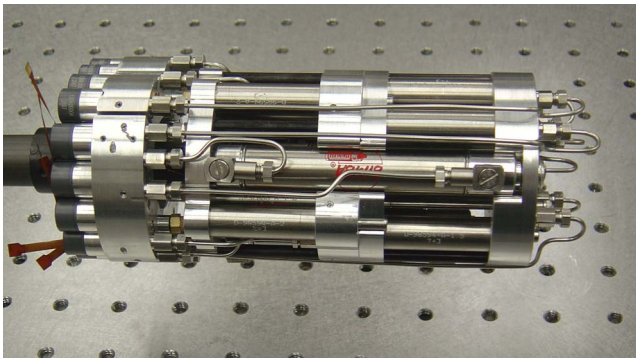

Fig. 11. Image of the forearm actuation unit mounted to the proximal forearm tube.

IV. ACTUATOR FORCE CONTROL

Preliminary functionality of the prosthesis has been tested and demonstrated with off-board supply of cold gas (nitrogen). Performance of the actuation unit was demonstrated with closed-loop control of the actuator output forces. Each actuator was controlled by a linear proportional and integral (PI) force control loop. Results for the two primary types of cylinders (double-acting for the wrist and single-acting for the hand tendons) are shown in Figs. 12-15. Figure 12 shows the step response for the double-acting cylinders (to indicate bandwidth and steady-state error), while Fig. 13 shows a slow (0.25 Hz) sinusoidal response, to indicate continuous tracking capability. Figures 14 and 15 show the same step and sinusoidal responses for the single acting cylinders. Note that the commands are (by necessity) always positive for the single-acting cylinders.

Note that the closed-loop force control bandwidth of the cylinders, which is approximately three Hertz, is limited by the bandwidth of the servovalves, which in turn is limited by the maximum speed of the brushless gearmotors. Specifically, when coupled to larger gearmotors (such as the Faulhaber 1319T006SR-IE2-400 with a 9:1 gearhead), the servovalves can provide order of magnitude higher bandwidths. Since a key design consideration of this actuation unit was minimizing its size and weight, the

smaller motors were used, which results in the closed-loop bandwidth of approximately three Hertz per actuator.

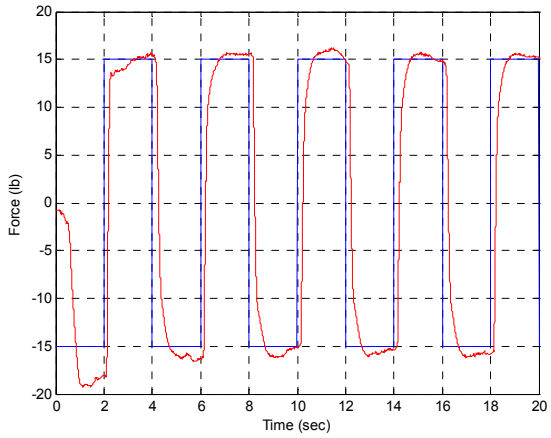

Fig. 12: Double-Acting Cylinder Force Control Performance (Step Response)

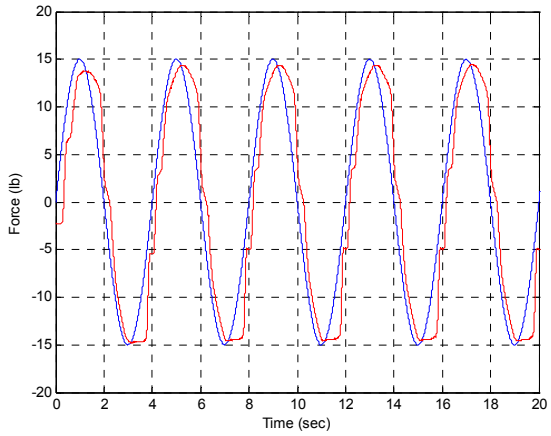

Fig. 13: Double-Acting Cylinder Force Control Performance (Sinusoidal Tracking)

V. Conclusion

A compact, 14 actuator forearm unit was designed, built, and tested for use in an anthropomorphic upper extremity prosthesis. Design of the forearm unit required the design and implementation of custom miniature servovalves and cylinder clusters. The forearm actuation unit has a mass of 930g (2.05 lb), which includes the weight of all components (excluding electronics and the liquid propellant cartridge), and is projected to deliver approximately 50% of the force, power, and energy of an anatomical human forearm.

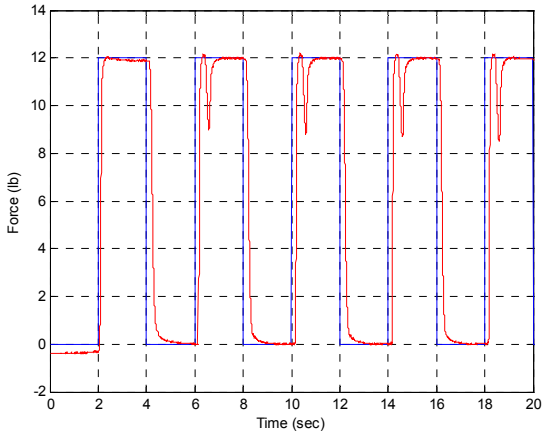

Fig. 14: Single-Acting Cylinder Force Control Performance (Step Response)

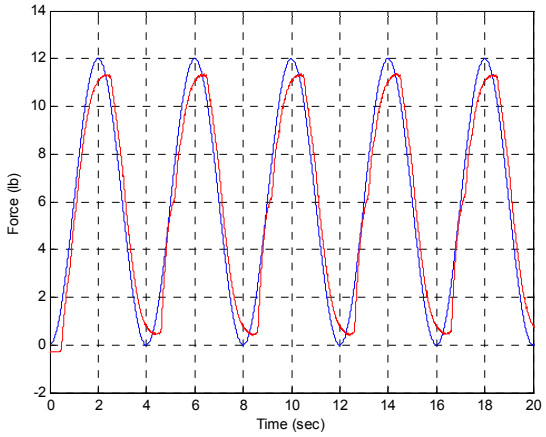

Fig. 15: Single-Acting Cylinder Force Control Performance (Sinusoidal Tracking)

References

[1] Fite K.B., Withrow, T.J., Wait, K. W. and Goldfarb, M. "A Gas-Actuated Anthropomorphic Transhumeral Prosthesis," *2007 IEEE International Conference on Robotics and Automation,* Roma, Italy, pp. 3748-3754, 2007.

[2] Goldfarb, M., Barth, E.J., Gogola, M.A. and Wehrmeyer, J.A., "Design and Energetic Characterization of a Liquid-Propellant-Powered Actuator for Self-Powered Robots," *IEEE/ASME Transactions on Mechatronics*, vol. 8, no. 2, pp. 254-262, 2003.

[3] Shields, B.L., Fite, K., and Goldfarb, M. "Design, Control, and Energetic Characterization of a Solenoid Injected Monopropellant Powered Actuator," *IEEE/ASME Transactions on Mechatronics*, vol. 11, no. 4, pp. 477-487, 2006.

[4] Fite, K.B., Mitchell, J., Barth, E.J., and Goldfarb, M. "A Unified Force Controller for a Proportional-Injector Direct-Injection Monopropellant-Powered Actuator," *ASME Journal of Dynamic Systems, Measurement and Control*, vol. 128, no. 1, pp. 159-164, 2006.

[5] Fite, K.B., and Goldfarb, M. "Design and Energetic Characterization of a Proportional-Injector Monopropellant-Powered Actuator," *IEEE/ASME Transactions on Mechatronics*, vol. 11, no. 2, pp. 196-204, 2006.

[6] Marquardt, E., "The Heidelberg pneumatic arm prosthesis," *Journal of Bone and Joint Surgery*, vol. 47 B, no. 3, pp. 425-434, 1965.

[7] Wilson, A.B.K., "Hendon pneumatic power units and controls for prostheses and splints," *Journal of Bone and Joint Surgery*, vol. 47 B, no. 3, pp. 435-441, 1965.

[8] Nickel V.L., Savill, D.L., Karchak, A., and Allen, J.R., "Synthetically powered orthotic systems," *Journal of Bone and Joint Surgery*, vol. 47 B, no. 3, pp. 458-464, 1965.
[9] Lambert, T.H., "An engineering appraisal of powered prostheses," *Journal of Bone and Joint Surgery*, vol. 49 B, no. 2, pp. 333-341, 1967.
[10] Burrows, C.R., Martin, D.J., and Ring, N.D., "Investigation into the dynamics and control of a pneumatically powered artificial elbow," *International Journal of Control*, vol. 15, no. 2, pp. 337-352, Feb. 1972.
[11] Kenworth, G. and Jolly, D.C., "Experience with the force-demand valve in controlling a pneumatically powered prosthesis," *Medical and Biological Engineering*, vol. 11, no. 1, pp. 90-94, Jan. 1973.
[12] Cool, J.C. and Pistecky, P.V., "A miniature gas-pressure valve," *Medical and Biological Engineering*, vol. 11, no. 6, pp. 771-779, Nov. 1973.